Bull. Mater. Sci., Vol. 38, No. 2, April 2015, pp. 461–465. © Indian Academy of Sciences.

Synthesis and spectroscopic characterization of palladium-doped titanium dioxide catalyst

FERESHTEH CHEKIN[1,*], SAMIRA BAGHERI[2] and SHARIFAH BEE ABD HAMID[2]

[1]Department of Chemistry, Ayatollah Amoli Branch, Islamic Azad University, Amol 678, Iran
[2]Nanotechnology & Catalysis Research Centre (NANOCAT), IPS Building, University Malaya, 50603 Kuala Lumpur, Malaysia

MS received 19 March 2014; revised 5 May 2014

Abstract. **In this work, we reported synthesis of palladium (Pd)-doped titanium dioxide (TiO_2) (Pd-TiO_2) nanoparticles by the sol–gel-assisted method. The synthesized Pd-doped TiO_2 nanoparticles were characterized using X-ray diffraction, transmission electronic microscopy, energy-dispersive spectroscopy, Fourier transform infrared (FT-IR) spectroscopy and voltammetry techniques. The analysis showed that particles are spherical in shape and pure anatase form with average size about 10 nm. To investigate the catalytic efficiency of Pd-TiO_2 nanoparticles, the hydrogen evolution reaction using the deposited film of Pd-TiO_2 nanoparticles on glassy carbon electrode (Pd-TiO_2/GCE) was studied in 0.1 M H_2SO_4 solution using linear scanning voltammetry. This study demonstrates the feasibility of using gelatin for the synthesis of Pd-TiO_2 catalyst.**

Keywords. **Pd-doped TiO_2 nanoparticles; gelatin; hydrogen evolution reaction.**

1. Introduction

Titanium dioxide (TiO_2) thin films have applications in optics and electronics because of their excellent properties, e.g. chemical and physical stability, high refractive index, high dielectric constants, high electrical resistance and interesting catalytic properties. The catalytic activity of TiO_2 is dependent on its crystal structure, crystal size distribution, surface roughness, surface hydroxyl group density, and so on.[1]

Highly dispersed nanoparticles of noble metals, such as Pt, Pd, Rh, Ru and Au in mesoporous supports as titania, alumina, silica are widely used as catalysts in organic synthesis, petrochemistry, etc. In a study concerning the photocatalytic activity of noble-metal-loaded TiO_2,[2–8] an ohmic contact is formed between the metal and semiconductor. Hence electrons can easily flow to the metal sites on TiO_2 under irradiation and the role of the metal is to act as an electron sink and thus to enhance the activity. However, it is difficult to introduce metal nanoparticles into mesopores by traditional impregnation methods, because they tend to deposit richly on outer surface of mesoporous materials and moreover it is difficult to control the loading amount by impregnation.[9]

Various deposition techniques such as electron beam evapouration,[10] metal organic chemical vapour deposition (MOCVD),[11] pulsed laser deposition,[12] reactive sputtering technique,[13] spray pyrolysis,[14] hydrothermal process[15] and sol–gel methods[16] have been used for production of TiO_2 thin films. Besides the above methods, sol–gel technique can be considered as the most influential technique for preparation of the mesoporous thin layers. It can provide good uniform composition and large specific areas via mild processing conditions.[17,18] High-purity and homogeneous oxide materials can be prepared by the sol–gel method, based on hydrolysis and polycondensation of metal-organic precursors, that allows an excellent compositional control. Sol–gel method easily allows the preparation of nanocomposite materials such as inorganic matrices in which a metal phase could be highly dispersed. Many studies deal with Pt dopant.[19–21] Concerning Pd doping, generally, its dispersion by the sol–gel method was made in SiO_2,[22,23] Al_2O_3[24,25] and in vitreous matrices.[4–8,26] There are few references so far regarding the use of Pd^{2+} as a dopant in the case of a sol–gel prepared TiO_2 matrix.

The hydrogen evolution reaction (HER) is an electrochemical process that has received wide attention because of its importance in both fundamental and technological electrochemistry such as fuel cell technology.[27,28] The search for new and less expensive alternative materials for HER has been a topic of current interest.[29–31] Deposition of Pt or Pd particles on the less expensive materials such as carbon supports reduced the cost of anode materials in the industrial applications.

In this paper, we report on construction of Pt-doped TiO_2 nanoparticles (Pd-TiO_2) by the green synthesis method. Techniques X-ray diffraction (XRD), transmission electronic microscopy (TEM), energy-dispersive spectrometer (EDS), Fourier transform infrared (FT-IR) spectroscopy and voltammetry were used to characterize the structure and property of the Pd-TiO_2. It was found that Pd-TiO_2 exhibited good catalytic activity toward the hydrogen evolution reaction.

*Author for correspondence (fchekin@yahoo.com)

2. Experimental

2.1 *Materials and apparatus*

Titanium tetraisopropoxide with purity 98% was obtained from Acros Organics. Palladium nitrate was purchased from Aldrich. Glacial acetic acid (100%) was purchased from Merck. Other reagents were of analytical grade and purchased from Aldrich or Merck and used as received without further purification.

Electrochemical measurements were performed with an Autolab Potentiostat/Galvanostat (Netherlands). The three-electrode system consists of a Pd-TiO_2/GCE as working electrode, Ag|AgCl|KCl_{3M} as the reference electrode and a platinum wire as an auxiliary electrode (Metrohm) were used in all voltammetric experiments. Bruker-D8 powder XRD was used for determination of crystal phase identification and estimation of the crystallite size. LEO-Libra 120 microscope was employed for Pd-TiO_2 nanoparticles TEM images. FT-IR spectroscopy studies were carried out with BRUKER FT-IR spectrometer. OXFORD (INCA Energy 400) EDS was used for the elemental analysis and chemical characterization of the sample. Electrochemical measurements were performed with an Autolab Potentiostat/Galvanostat (Netherlands).

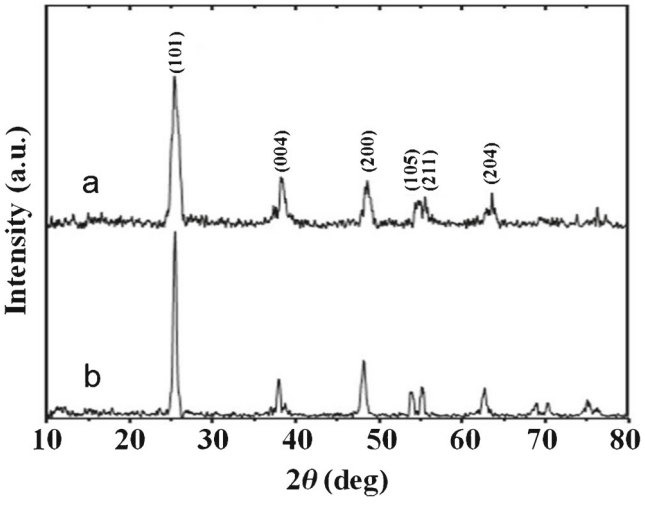

Figure 1. XRD patterns of (**a**) Pd-TiO_2 and (**b**) TiO_2.

2.2 *Synthesis of Pd-doped TiO_2 nanoparticles*

The precursor solution was prepared by dissolving titanium tetraisopropoxide (TTIP) in the glacial acetic acid (AA), followed by the addition of H_2O. The mol ratio of TTIP:AA:H_2O must be kept at 1:10:200. Gelatin solution was made by dissolving 3.0 g of gelatin in 100 ml of deionized water and stirred for 30 min at 60°C to achieve a clear gelatin solution. Then, the gelatin solution was added into the precursor solution. Then, 10 ml of 1 M Pd solution was added drop wise into the precursor solution for a few minutes. The solution was dried at the temperature of 80°C overnight. The dried gel was grinded and calcined in a muffle furnace at 500°C for 5 h.

2.3 *Fabrication of Pd-TiO_2/GCE*

Prior to modification, the bare GCE was polished on chamois leather with 0.05 μm alumina powder. Then it was thoroughly sonicated in deionized water and absolute ethanol, respectively. One milligram of synthesized Pd-TiO_2 was dispersed in 5 ml dimethyl formamide (DMF) with the aid of ultrasonic agitation. The cleaned GCE was coated by casting 5 μl of the Pd-TiO_2 solution and dried at 50°C in an oven air to remove the solvent.

3. Results and discussion

3.1 *X-ray diffraction and FT-IR spectroscopy*

Figure 1 shows XRD patterns of TiO_2 and Pd-TiO_2 powders calcined at 500°C under air for 5 h. From the wide-angle XRD pattern, the titania samples exist only in anatase phase, with their characteristic diffraction peaks of 2θ values at about 25.4 (101), 37.9 (004), 48.2 (200), 54.0 (105), 55.1 (211) and 62.9 (204), respectively. In consequence, the prepared Pd/TiO_2 (pattern a) and TiO_2 (pattern b) powders are well-crystallized pure anatase form. From the maximum diffraction peak at figure 1 by Scherrer's formula ($D = K\lambda/\beta\cos\theta$, where D is the crystallite size, K the Scherrer constant usually taken as 0.89, λ the wavelength of the X-ray radiation (0.15418 nm for Cu Kα), and β the full-width at half-maximum of diffraction peak measured at 2θ, the average particle sizes of pure Pd-TiO_2 and TiO_2 powders for (101)

Table 1. Compared parameters of Pd-TiO_2 synthesized using different methods.

Method	Template	Particle size (nm)	Synthesized temperature (°C)	Reference
Sol–gel dip coating	Pluronic P123[a]	7.1	500	8
Magnetron sputtering	—	23.4	900	7
Sol–gel dip coating	—	30.7	500	6
Electrospinning	Polyvinyl pyrrolidone	25.0	600	32
Sol–gel	Gelatin	10.0	500	This work

[a]Poly-(ethylene oxide) poly-(propylene oxide) poly-(ethylene oxide).

plane, are about 10 and 15 nm, respectively. In comparison with XRD pattern of pure TiO_2, Pd loaded on TiO_2 surface nearly has no influence on crystalline structure. Pd phase has not been detected in the XRD patterns of Pd-TiO_2 powders, possibly because the Pd content on TiO_2 surface is not enough to form clearly crystalline. A comparison of particle size, temperature and synthesis method of Pd-TiO_2 synthesized in this work with those already reported in literatures is shown in table 1. As shown, parameters are comparable with other results.

Figure 2 shows the FT-IR spectra of Pd-TiO_2 (pattern a) and TiO_2 (curve b) nanoparticles in range of 400–4000 cm^{-1} which were synthesized via the sol–gel method. In undoped TiO_2, the peaks at 431 and 701 cm^{-1} are for O–Ti–O bonding. The band centered at 1608 cm^{-1} is characteristic of δ-H_2O bending. The broad absorption bands between 400 and 800 cm^{-1} are mainly ascribed to Ti–O and O–Ti–O– flexion vibration. However, the vibration bands between 1300 and 4000 cm^{-1} are mainly assigned to the chemisorbed and/or physisorbed H_2O and CO_2 molecules on the surface of the compound. When metal ions are doped to the surface of TiO_2, the absorption band transforms and simultaneously new absorption band appears. Upon addition of dopant, a small shift was detected for the stretching vibration of Ti–O.[33]

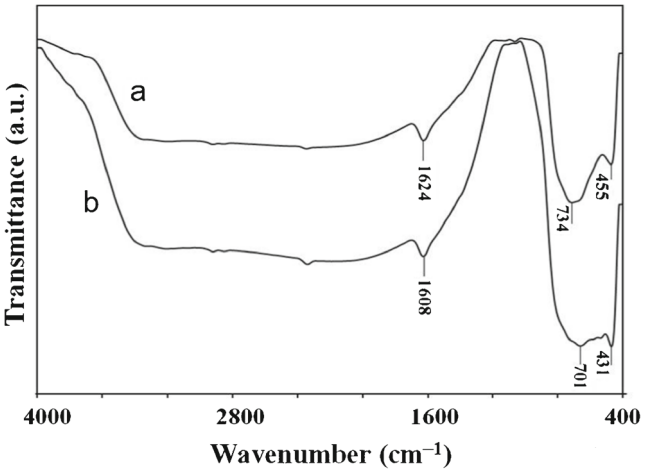

Figure 2. FT-IR patterns of (**a**) Pd-TiO_2 and (**b**) TiO_2.

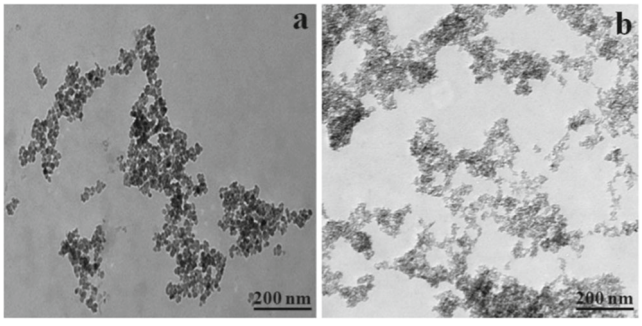

Figure 3. TEM images of (**a**) TiO_2 and (**b**) Pd-TiO_2.

3.2 *Transmission electronic microscopy and energy-dispersive spectroscopy*

TEM micrographs of TiO_2 and Pd-TiO_2 are shown in figure 3. Electron microscopy analyses reveal that TiO_2 (image a) and Pd-TiO_2 (image b) samples exhibit similar morphology. As shown in TEM images, particle size of the Pd-TiO_2 is smaller than TiO_2. Energy dispersive X-ray spectroscopy (EDS) of Pd-TiO_2 is shown in figure 4 which confirms the existence of Ti, O and Pd with weight percent.

3.3 *Electrochemical behaviour of Pd-TiO_2/GCE*

The cyclic voltammetry (CV) curve of Pd-TiO_2/GCE in 0.1 M H_2SO_4 solution at 50 mV s^{-1} in a potential window of −0.3 to 1.2 V (figure 5) exhibits a typical H^+ ion electro-adsorption/desorption region, a double layer charging current region, a Pd pre-oxidation region and a Pd oxy-species reduction region. In the proton adsorption/desorption region, current peaks observed at 0 V and −0.1 V, which corresponds

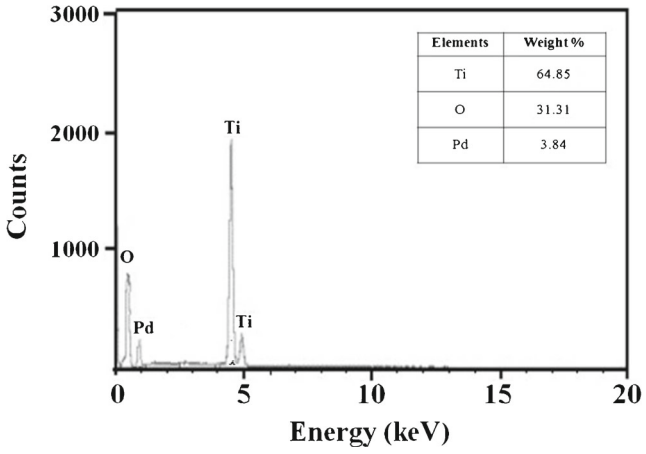

Figure 4. EDAX pattern of Pd-TiO_2.

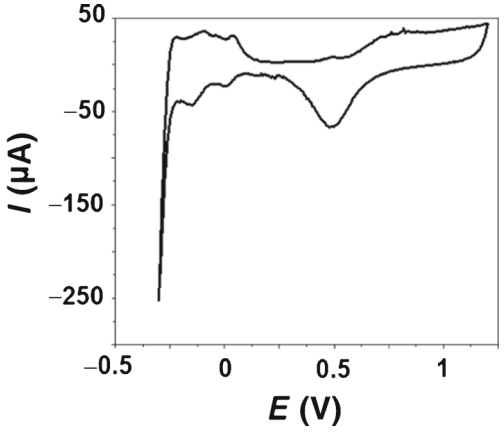

Figure 5. Cyclic voltammogram of Pd-TiO_2/GCE in 0.1 M H_2SO_4 solution at scan rate 50 mV s^{-1}.

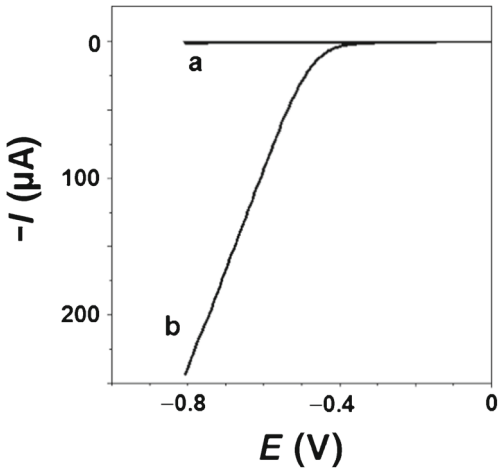

Figure 6. Linear sweep voltammograms of (**a**) bare GCE and (**b**) Pd-TiO_2/GCE in 0.1 M H_2SO_4 at a scan rate of 5 mV s^{-1}.

to polycrystalline Pd, confirmed the existence of Pd, as evidenced by EDS, FT-IR and TEM. The surface concentration of the electroactive Pd on Pd-TiO_2/GCE, Γ (in mol cm^{-2}), can be estimated using the equation[34]

$$\Gamma = Q/nFA, \tag{1}$$

where Q is the charge consumed in Coulombs, obtained from integrating the anodic (or cathodic) peak area in cyclic voltammograms under the background correction. The average Γ value of $(1.44 \pm 0.89) \times 10^{-10}$ mol cm^{-2} was obtained.

3.4 *Electrocatalytic behaviour of Pd-TiO_2/GCE*

To evaluate the activity of the Pd-TiO_2 catalyst, the electrocatalysis of HER was studied by linear scanning voltammetry (LSV), and results are shown in figure 6. As expected, the electrocatalytic activity improves at surface of Pd-TiO_2/GCE (curve b) as though the onset potential of HER occurs at about −0.4 V *vs.* Ag|AgCl|KCl_{3M} and is indicated by an abrupt increase of the cathodic current. Also, the experiment concerning HER on a bare GCE (curve a) was studied as shown in figure 6. As can be seen, at the same current density, the overpotential of HER at Pd-TiO_2/GCE is lower than that at GCE.

4. Conclusion

In summary, we demonstrated that Pd-doped TiO_2 nanoparticles can be easily formed by the sol–gel method. The analysis showed that particles are spherical in shape and pure anatase form with average size about 10 nm. To investigate the catalytic efficiency of Pd-TiO_2, the hydrogen evolution reaction was studied using the deposited film of Pd-TiO_2 on glassy carbon electrode in 0.1 M H_2SO_4 solution using LSV. The electrocatalytic activity improves at surface of Pd-TiO_2/GCE as though the onset potential of HER occurs at about −0.4 V *vs.* Ag|AgCl|KCl_{3M} and is indicated by an abrupt increase of the cathodic current.

References

1. Sonawane R S, Kale B B and Dongare M K 2004 *Mater. Chem. Phys.* **85** 52
2. Chen H W, Ku Y and Kuo Y L 2007 *Water Res.* **41** 2069
3. Huang M, Xu C, Wu Z, Huang Y, Lin J and Wu J 2008 *Dyes Pigm.* **77** 327
4. Ranjit K T, Varadarajan T K and Viswanathan B 1996 *J. Photochem. Photobiol. A: Chem.* **96** 181
5. Crisan D, Drăgan N, Crisan M and Răileanu M 2009 *J. Phys. Chem. Solids* **69** 2548
6. Mardare D, Iftimie N, Crişan M, Răileanu M, Yildiz A, Coman T, Pomoni K and Vomvas A 2011 *J. Non-Cryst. Solids* **357** 1774
7. Kim S C, Heo M C and Hahn S H 2005 *J. Kor. Phys. Soc.* **47** 700
8. Yarmand B and Sadrnezhaad S K 2010 *Optoelectron. Adv. Mater. Rapid Commun.* **4** 1572
9. Yuan S, Sheng Q, Zhang J, Chen F, Anpo M and Dai W 2006 *Catal. Lett.* **107** 19
10. Bhattacharyya D, Sahoo N K, Thakur S and Das N C 2000 *Thin Solid Films* **360** 96
11. Zhang X W, Zhou M H and Lei L C 2006 *Catal. Commun.* **7** 427
12. Gyorgy E, Socol G, Axente E, Mihailescu I N, Ducu C and Ciuca S 2005 *Appl. Surf. Sci.* **247** 429
13. Mardare D, Nica V, Teodorescu C M and Macovei D 2007 *Surf. Sci.* **601** 4479
14. Oja I, Mere A, Krunks M, Nisumaa R, Solterbeck C H and Es-Souni M 2006 *Thin Solid Films* **515** 674
15. Kambe S, Murakoshi K, Kitamura I, Wada Y, Yanagida S, Kominami H and Kera Y 2000 *Sol. Energy Mater. Sol. Cells* **61** 427
16. Cernigoj U, Stangar U L, Trebxe P, Kraxovec U O and Gross S 2006 *Thin Solid Films* **495** 327
17. Yun H, Miyazawa K, Honma I, Zhou H and Kuwabara M 2003 *Mater. Sci. Eng. C* **23** 487
18. Liu K, Zhang M, Shi K and Fu H 2005 *Mater. Lett.* **59** 3308
19. Facchin G, Carturan G, Campostrini R, Gialanella S, Lutterotti L, Armelao L, Marci G, Palmisano L and Sclafani A 2000 *J. Sol–Gel Sci. Technol.* **18** 29
20. López T, Gómez R, Pecci G, Reyes P, Bokhimi X and Novaro O 1999 *Mater. Lett.* **40** 59
21. López T, Gómez R, Romero E and Schifter I 1993 *React. Kinet. Catal. Lett.* **49** 95
22. López T, Morán M, Navarrete J, Herrera L and Gómez R 1992 *J. Non-Cryst Solids* **147&148** 753
23. López T, Bosch P, Navarrete J, Asomoza M and Gómez R 1994 *J. Sol–Gel Sci. Technol.* **1** 193
24. Othman M R and Sahadan I S 2006 *Micropor. Mesopor. Mater.* **91** 145

25. Noh J, Yang O B, Kim D H and Woo S I 1999 *Catal. Today* **53** 575
26. Carturan G, Facchin G, Gottardi V, Guglielmi M and Navazio G 1982 *J. Non-Cryst. Solids* **48** 219
27. Trasatti S 1991 *Electrochim. Acta* **36** 225
28. Xu Y H, He G R and Wang X L 2003 *Int. J. Hydrogen Energy* **28** 961
29. Shibli S M A and Dilimon V S 2007 *Int. J. Hydrogen Energy* **32** 1694
30. Karimi Shervedani R and Madram A R 2007 *Electrochim. Acta* **53** 426
31. Xu Y, Chen C, Wang X and Wang Q 2007 *Int. J. Hydrogen Energy* **32** 537
32. Moon J, Park J Ah, Lee Su J, Zyung T and Kim D 2010 *Sens. Actuators B* **149** 301
33. Zhang X, Zhou G, Xu J, Bai G and Wang L 2010 *J. Solid State Chem.* **183** 1394
34. Laviron E 1979 *J. Electroanal. Chem.* **100** 263